Ordered Structure in Blends of Block Copolymers. 3. Self-Assembly in Blends of Sphere- or Cylinder-Forming Copolymers†

Satoshi Koizumi,‡ Hirokazu Hasegawa, and Takeji Hashimoto*

Division of Polymer Chemistry, Graduate School of Engineering, Kyoto University, Kyoto 606-01, Japan

Received November 29, 1993; Revised Manuscript Received April 26, 1994•

ABSTRACT: Ordered structures of binary mixtures of poly(styrene-*block*-isoprene) diblock copolymers (SI) were studied with transmission electron microscopy and small-angle X-ray scattering. In the case when $f_\alpha \cong f_\beta \cong 0.8$ or $f_\alpha \cong 1 - f_\beta \cong 0.7$ and $r \equiv N_\alpha/N_\beta \leq 2$, the two copolymers, designated α and β, are found to be mixed at a molecular level for all blending compositions, resulting in a single domain morphology (i.e., spherical microdomains packed in a cubic lattice, hexagonally packed cylindrical microdomains, or alternating lamellar microdomains). Here f_K and N_K are the volume fraction of one of the block chains (e.g., polystyrene) and the total degree of polymerization of the Kth copolymer ($K = \alpha$ or β, $N_\alpha > N_\beta$). Even in the case when $f_\alpha \cong f_\beta \cong 0.8$, if $r \geq 7$, α and β are found to be partially miscible. They phase-separate into large spheres rich in α and small spheres composed of almost pure β for the composition (Φ_α) of α component satisfying $\Phi_\alpha \leq \Phi_{\alpha,C} \cong 0.8$. The phase separation was proposed to result from the "*fluctuation-induced segregation effect*". On the other hand, in the case when $f_\alpha \cong 1 - f_\beta = 0.8$ (or 0.2 and $r \cong 1.2$), the mixtures are found to form a modulated (or superlattice) structure having a spatial arrangement of α-rich and β-rich domains with a characteristic length scale of microns. Each domain rich in α or β has the microdomain structure characteristic of the copolymers α or β with a characteristic length scale of nanometers. The superlattice structure was proposed to originate from the macrophase separation between α and β and subsequent microphase separation induced in the regions rich in α and β copolymers.

I. Introduction

In the previous works of this series,[1,2] we explored a miscibility criterion and self-assembled structures in binary mixtures of the poly(styrene-*block*-isoprene) diblock copolymers (S-I). The two copolymers $(S\text{-}I)_\alpha$ and $(S\text{-}I)_\beta$ having $f_\alpha \cong f_\beta \cong 0.5$ were examined, f_K being the composition of the polystyrene block chain (PS) for the Kth S-I copolymer (K = α or β). They were totally miscible at the molecular level to give a single microdomain morphology in the segregation limit, in the case of $r \equiv N_\alpha/N_\beta \leq 5$. Here N_K is the total degree of polymerization for the Kth copolymer ($K = \alpha$ or β, $N_\alpha > N_\beta$). However, in the case of $r \geq 10$, two copolymers were found to be partially miscible, undergoing the *macrophase separation* into the regions rich in α and those rich in β for the blend composition Φ_α satisfying $\Phi_{\alpha,CS} \leq \Phi_\alpha \leq \Phi_{\alpha,CL}$. This *macrophase separation* was proposed to occur as a consequence of the *microphase separation* of the copolymers.

In part 2 of this series,[2] we explored, in detail, the morphology of the macrophase-separated domains, especially the morphology at the interface in which the two coexisting microdomains rich in α and β are commensurate with each other. The morphology was qualitatively interpreted on the basis of the "*macrophase separation induced by microphase separation*" which in turn was proposed to be triggered by the "fluctuation-*induced segregation effect*": when the mixtures become thermodynamically unstable and the amplitude of the concentration fluctuations increases, the small copolymers $(S\text{-}I)_\beta$ are put in the fields rich in polystyrene block (PS_α) or polyisoprene block (PI_α) of the large copolymer $(S\text{-}I)_\alpha$; viz., $(S\text{-}I)_\beta$ polymers feel as if they are put in the field of homopolymers PS_α or PI_α, and hence they are subjected to segregation from the microdomains of $(S\text{-}I)_\alpha$.

Table 1. Molecular Characteristics of Block Copolymers

specimen code	$10^{-4} M_n$	$10^{-3} N_w$	M_w/M_n	PS/PI wt/wt	PS/PI vol/vol	morphology
HS11	122.0	17.0	1.31	80/20	78/22	sphere
B2	17.6	2.30	1.26	85/15	83/17	sphere
B1	8.2	1.05	1.22	83/17	81/19	cylinder
TOKI4	9.4	1.67	1.30	20/80	18/82	cylinder
BSI9	22.4	2.53	1.00	67/33	64/36	cylinder
HK5	18.2	3.01	1.25	29/71	26/74	cylinder

In this paper we further extend the studies along this line on the miscibility and self-assembled structures in the binary S-I copolymers having $f_{PS} \cong 0.64$–0.83 or 0.17–0.26 and hence showing either spherical or cylindrical microdomains.

II. Experimental Method

A. Specimens. S-I block copolymers studied in this experiment were prepared by sequential living anionic polymerization with *sec*-butyllithium as the initiator and benzene (for TOKI4) or tetrahydrofuran (for the others) as the solvent. Table 1 summarizes the characteristics of the copolymer samples. An important feature of these S-I samples is that they are asymmetric block copolymers and all of them have the volume fraction of one component about 0.7–0.8, thus forming cylindrical or spherical microdomain morphologies. A major component is PI for HK5 and TOKI4 and PS for the others.

We studied binary mixtures of B2/B1 and HS11/B2 having similar f_{PS} ($\cong$0.2) but different r (2.15 and 6.90, respectively) and those of BSI9/HK5 and B2/TOKI4 having different f_{PS}. The blend specimens were prepared by dissolving the polymer mixtures to make 5.0 wt % solutions in toluene, a neutrally good solvent for both PS and PI, and by evaporating the solvent very slowly over 2 weeks at 30 °C in Petri dishes. The film specimens thus obtained were further dried in a vacuum oven until constant

† Presented in part at the 38th Symposium of the Society of Polymer Science, Japan, October 1989, *Polym. Prepr. Jpn.* 1989, *38*, 4161–4163.

‡ Present address: Neutron Scattering Laboratory, Department of Materials Science and Engineering, Japan Atomic Energy Research Institute, Tokaimura, Ibaraki 319-11, Japan.

• Abstract published in *Advance ACS Abstracts*, June 1, 1994.

0024-9297/94/2227-4371$04.50/0

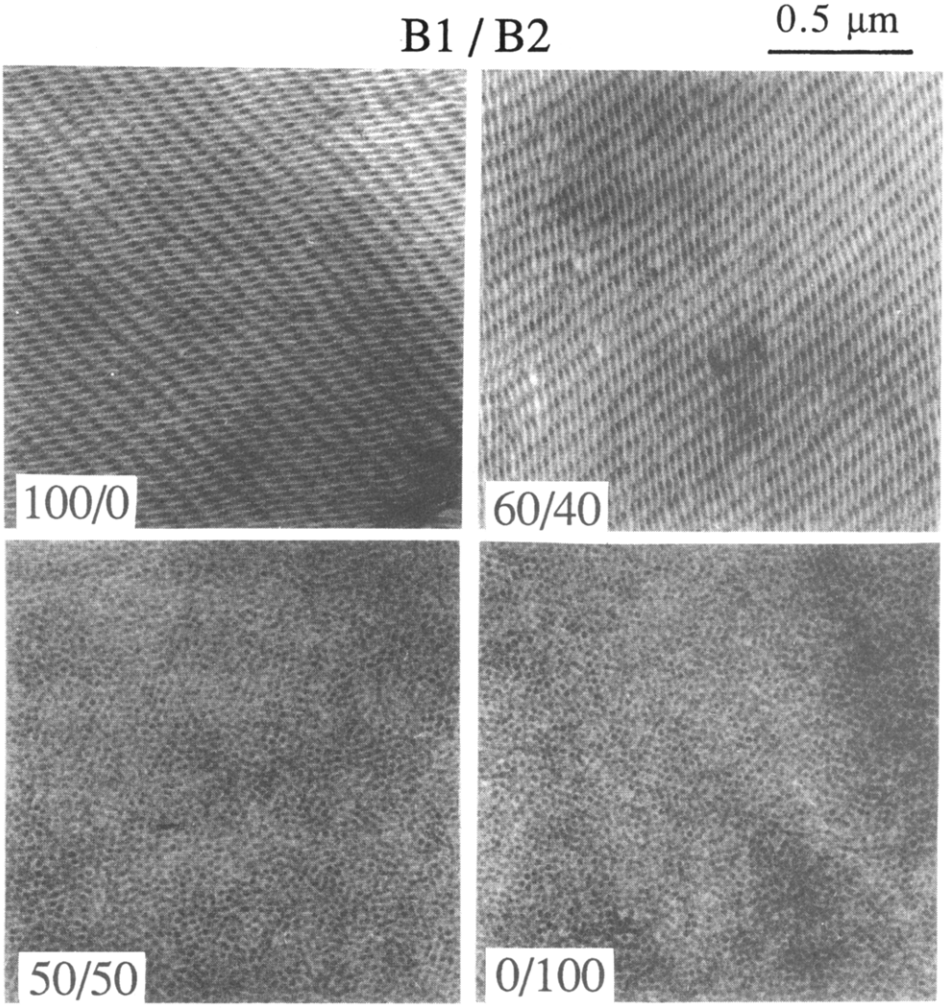

Figure 1. Transmission electron micrographs of ultrathin sections of B1/B2 mixtures stained with osmium tetraoxide. Neat B1 (100/0) and the 60/40 mixture show the hexagonally packed PI cylindrical microdomains in the matrix of PS block chains. On the other hand, neat B2 (0/100) and the 50/50 mixture show the PI spherical microdomains in the matrix of PS block chains. Macrophase separation was not observed in any mixtures. The morphological transition from cylinder to sphere was observed at a composition between 60/40 and 50/50.

weight was attained. The thickness of the cast films was ca. 0.5 mm. The specimens thus obtained were further annealed at 150 °C for 2 h in a vacuum oven.

B. Electron Microscopy. The microdomain structures formed in the films of the binary mixtures were examined by transmission electron microscopy (TEM). TEM observation was done with a Hitachi H-600S transmission electron microscope at 100-kV accelerating voltage. To prepare the test specimens, the blend films were first stained with osmium tetraoxide (O_SO_4) vapor and embedded in epoxy resin. The ultrathin sections of ca. 50-nm thickness were obtained by using an LKB 4800A Ultrotome with a glass knife at room temperature.

C. Small-Angle X-ray Scattering. The microdomain structures were investigated by small-angle X-ray scattering (SAXS) (wavelength $\lambda = 0.154$ nm) using a 12-kW rotating anode X-ray generator operated at 50 kV and 200 mA, a 1.5-m SAXS camera with a graphite monochromator, and a one-dimensional position sensitive proportional counter. The SAXS profiles were corrected for the air scattering, the absorption, and the background scattering due to thermal diffuse scattering (TDS). The profiles were further corrected for the slit-height and slit-width smearing effects.

III. Experimental Results

A. TEM Observation. Figure 1 shows typical TEM micrographs for the binary mixtures of B1/B2. The 100/0 specimen (neat B1) exhibits a cylindrical microdomain morphology, with the dark PI cylinders stained with O_SO_4 being dispersed in the bright matrix of unstained PS block chains. On the other hand, the 0/100 specimen (neat B2) exhibits a spherical microdomain morphology with the PI spheres dispersed in the matrix of unstained PS. Similarly, the 50/50 mixture shows a uniform structure of spherical microdomains with a monodispersed diameter all over the specimen. This means that the two different kinds of block copolymers were mixed at the molecular level to form a single spherical microdomain. On the other hand, the 60/40 mixture shows a uniform structure of hexagonally packed cylindrical microdomains with a monodispersed diameter and domain spacing all over the specimen, indicating that the two copolymers are mixed to form a single domain morphology. It should be noted that only one type of microdomain morphology was observed in each composition and that there was an abrupt change in morphology from the cylindrical to the spherical one at a composition of $(S\text{-}I)_\beta/(S\text{-}I)_\alpha$ between 60/40 and 50/50.

Figure 2 shows TEM micrographs of the neat SI copolymers HK5 (part a) and BSI9 (part c) and that of their 50/50 wt %/wt % mixture (part b). HK5 shows hexagonally packed PS cylinders in the PI matrix, while BSI9 shows the hexagonally packed PI cylinders in the PS matrix. The 50/50 mixture uniformly shows the alternating lamellar microdomains of the PS and PI block chains everywhere in the sample space. This implies the two copolymers are mixed at the molecular level to form the single microdomain morphology with a long-range spatial order.

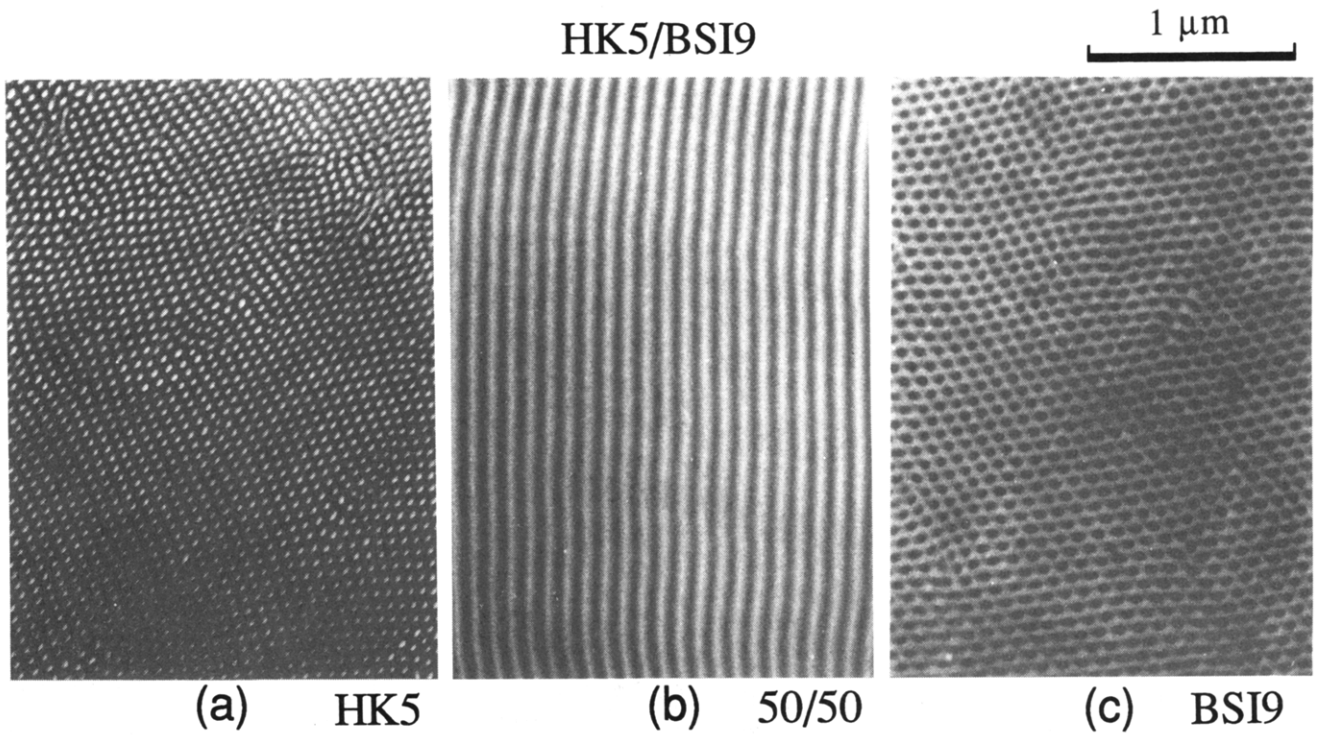

Figure 2. Transmission electron micrographs of ultrathin sections of HK5/BSI9 mixtures stained with osmium tetraoxide: (a) neat HK5, (b) 50/50 mixture, and (c) neat BSI9. HK5 shows the hexagonally packed PS cylinders in the matrix of the PI block chains, while BSI9 shows the hexagonally packed PI cylinders in the matrix of PS block chains. The 50/50 mixture shows the alternating lamellar microdomains in which both HK5 and BSI9 block chains are mixed uniformly at a molecular level.

Figure 3 shows typical TEM micrographs obtained for the binary mixtures of B2/HS11. Neat B2 and HS11 both form spherical microdomains of PI block chains in the matrix of PS block chains, but their average domain diameters and domain spacings are quite different. In the 20/80 mixture only one type of spherical microdomains with an average diameter and an average spacing in between those of the neat copolymers is observed. In contrast, the 30/70 mixture shows the coexistence of two types of spherical microdomains: large ones having the average diameter close to that of the 20/80 mixture and small ones having the average diameter close to that of neat B2. The large and small spheres are uniformly dispersed over the scale of a few microdomains. This means that the large and small copolymers segregate into the respective spheres, but this segregation does not extend to the macroscopic level, in such a way that they form macrodomains packed with large spheres and macrodomains with small spheres (see Figure 9 later) (*the "local-scale" phase separation*). The local-scale phase separation without the macrophase separation similar to the 30/70 mixture was observed in the TEM images of the mixtures with the compositions from 40/60 to 90/10. The average distance between the adjacent large spheres depends on the blend composition or the fraction of small spheres composed of B2. The 90/10 mixture shows such a unique structure that the large spheres are randomly distributed in the ordered cubic lattice composed of the small spheres.

Figure 4 shows the TEM image of the 30/70 mixture of TOKI4/B2. Neat TOKI4 has a microdomain structure of PS cylinders hexagonally packed in the PI matrix, though not shown here. The image of the mixture is complicated. It shows the coexistence of the two macrophases: one which forms the dispersed domain has a microdomain morphology similar to that of neat TOKI4, i.e., PS cylinders dispersed in the PI matrix, and the other which forms the matrix has a microdomain morphology identical to that of neat B2, i.e., PI spheres in the PS matrix (Figure 1). The image shows the macrophase separation between the two copolymers and the microphase separation within the macrophase-separated domains rich in copolymers α and β. The interplay of the two kinds of phase separation produces a "*modulated*" or "*superlattice*" *structure* with dual morphological entities having two characteristic length scales: the micron-scale structure developed by the macrophase separation and the nanometer-scale developed by the microphase separation.

B. SAXS Profiles. Figure 5 shows SAXS profiles for the binary mixtures of B1/B2. The profile of neat B1 shows the interdomain interference maxima and shoulder at wavenumbers in the ratios of $1, 3^{1/2}, 4^{1/2}, 7^{1/2}$, and $12^{1/2}$, as marked by thin arrows indicating hexagonally packed cylindrical domains. The broad scattering maxima marked by thick arrows originate from the form factor of the isolated cylinders. The peak positions, q_{mi}, give the average radius of the cylinders, R,

$$q_{mi}R = 4.98, 8.364, 11.46, \ldots \quad (1)$$

for $i = 1, 2, 3, \ldots$, respectively. Here q_{mi} is the scattering vector given by

$$q_{mi} = (4\pi/\lambda) \sin(\theta_{mi}/2) \quad (2)$$

with θ_{mi} being the scattering angle for the ith maximum from the form factor of the PI cylinders.

The profile of neat B2 has sharp and broad peaks or shoulders at wavenumbers in the ratios of $1, 2^{1/2}$, and $3^{1/2}$, as marked by thin arrows in Figure 5. These peaks imply the spherical microdomains pakced in a simple cubic (SC) lattice or a body-centered-cubic (BCC) lattice (see section IV.A below). The broad peaks marked by thick arrows are due to the form factor of the PI spheres. These peaks are located at q_{mi} which is approximately given by the

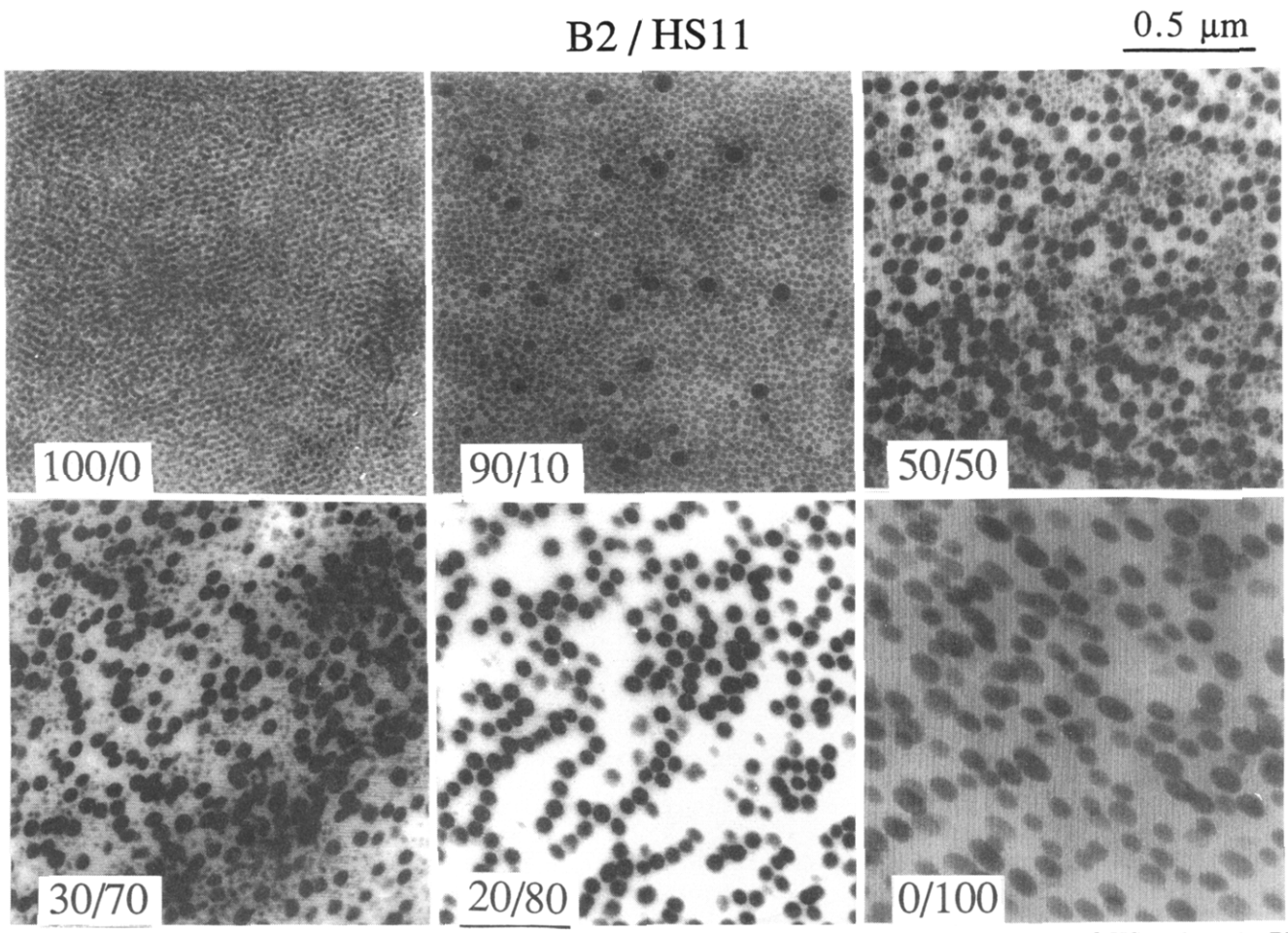

Figure 3. Transmission electron micrographs of ultrathin sections of B2/HS11 mixtures. Both neat B2 and HS11 show the PI spherical microdomains in the matrix of PS block chains. The 20/80 mixture shows only one kind of spherical microdomain whose size is in between those of neat B2 and HS11, while the mixtures from 30/70 to 90/10 show the two kinds of spherical microdomains whose sizes are close to those of neat B2 and HS11.

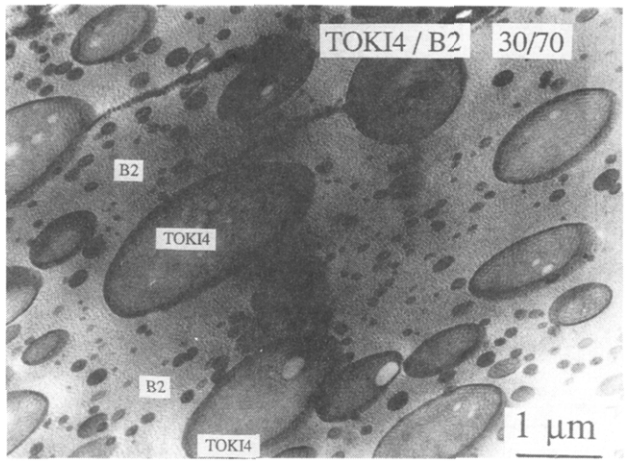

Figure 4. Transmission electron micrograph of an ultrathin section of the 30/70 mixture of TOKI4/B2 showing the coexistence of two macrophases. The TOKI4-rich domains composed of PS cylinders in the matrix of the PI block chains are dispersed in the B2-rich matrix composed of PI spheres in the matrix of the PS block chains.

following equation,

$$q_{mi}R = 5.765, 9.111, 11.22, \ldots \quad (3)$$

for $i = 1, 2, 3, \ldots$ respectively, where R is an average radius of the PI spheres and θ_{mi} is the scattering angle for the ith maximum from the PI spheres.

With increasing B2 content in B1/B2 mixtures from 100/0 to 55/45, the SAXS profiles hardly changed and remained nearly identical to that of neat B1. This implies that the cylindrical microdomains are formed in all of these mixtures, which is consistent with the TEM observation shown in Figure 1. In contrast, the SAXS profiles for the mixtures with the composition B1/B2 ranging from 50/50 to 0/100 (neat B2) are quite different from those from 100/0 (neat B1) to 55/45 but similar to that of neat B2. This implies that the B1/B2 mixtures with compositions from 50/50 to 0/100 have spherical microdomains, which is also consistent with the TEM observation in Figure 1.

Figure 6 shows SAXS profiles obtained for the binary mixtures of B2/HS11. The SAXS profile of neat HS11 exhibits several broad peaks, as indicated by long arrows marked with the numbers 1 to 4. These peaks are due to the form factor from isolated spherical microdomains composed of the PI block chains. The wavenumber q_{mi} of the peak positions satisfies eq 3. In this case, the interdomain interference maxima cannot be observed because they are out of the q range of our SAXS instrument. With increasing weight fraction of the small block copolymer B2, these peak positions first shift toward larger q up to 20% of B2 (20/80), and then stay constant from 30% (30/70) to 50% of B2 (50/50). Here it should be pointed out that the 30/70 mixture of B2/HS11 is the system giving rise to the coexistence of two types of spherical microdomains, as shown by the TEM image in Figure 3. However, the contribution of the small spheres composed of B2 to the net scattering is small compared to that of the large spheres, so that its effect is difficult to discern. The broad maxima marked by thick short arrows with circled numbers 1–3 in the profiles of 100/0

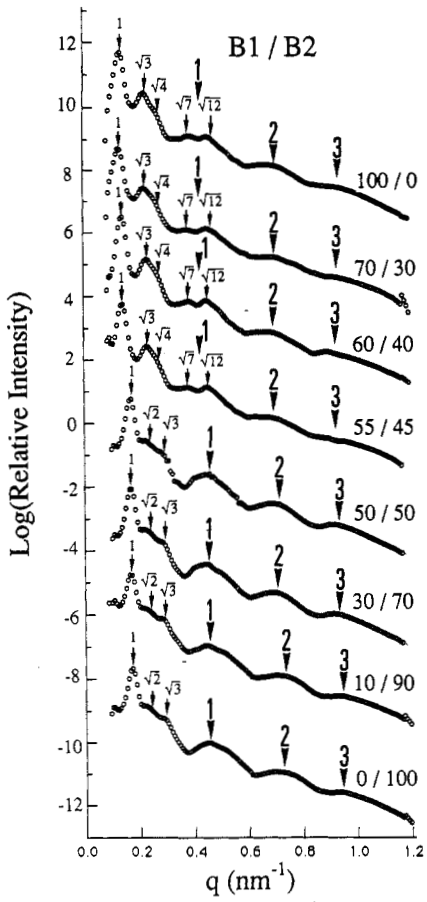

Figure 5. SAXS profiles obtained for the B1/B2 mixtures with the compositions 100/0, 70/30, 60/40, 55/45, 50/50, 30/70, 10/90, and 0/100. The mixtures from 100/0 to 55/45 show the scattering profiles typical of the cylindrical microdomains, while the mixtures from 50/50 to 0/100 show the scattering profiles typical of the spherical microdomains. There is a sharp morphological transition between 55/45 and 50/50.

to 50/50 mixtures of B2/HS11 reflect the maxima in the form factor from the isolated spheres of B2 (see discussion related to Figure 12 in section IV.C). They again satisfy eq 3. Upon a further increase of B2, greater than or equal to 70%, the broad maxima from the isolated spheres of HS11 marked by the long arrows cannot be identified because they are outweighed by the scattering from B2.

For the mixtures of B2/HS11 from 50/50 to 70/30, the SAXS profiles are distorted because of the balance of the scattering from the large and small spherical microdomains, as appeared from the TEM images shown in Figure 3. In the SAX profiles for the mixtures of B2/HS11 from 100/0 to 80/20, the small-angle peaks at the wavenumbers in the ratios of 1, $2^{1/2}$, and $3^{1/2}$, as marked by thin short arrows, and the peaks at large wavenumbers, as marked by thick short arrows with circled numbers 1–3, reflect respectively intersphere interference maxima and the form factor of isolated spheres of the small molecular weight copolymer B2. The SAXS profiles are getting similar to that of neat B2 with a further increase of the composition B2, especially so for mixtures 80/20 and 90/10. It is interesting to note that the first-order interparticle interference peak (the thin short arrow) shifts toward a larger angle with increasing B2, but the first-order peak in the form factor of the spheres (the thick short arrow) does not change. This indicates that the size of the small spheres stays constant but the intersphere distance of the small spheres becomes shorter with the decreasing fraction of the large spheres or the large molecular weight copolymers α; viz., *the small spheres tend to be packed more compactly with the decreasing fraction of the large spheres*, or a small fraction of the large spheres tends to loosen the packing of the small spheres.

IV. Discussion

A. Miscible Blends of B1/B2 with $r < r_c$ and $f_\alpha \cong f_\beta \cong 0.8$: Microphase Separation Only. The mixture B1/B2 has a very small mismatch in the composition of f_{ps} (the composition difference $|f_\alpha - f_\beta| = 0.02$) such that they cannot be unstable for the macrophase separation. The stability analysis based upon RPA indicates that the spinodal point for the macrophase transition for the block copolymers in a disordered state is given by

$$2\chi_{eff,s} = 1/(N_\alpha\Phi_\alpha) + 1/(N_\beta\Phi_\beta) \quad (4)$$

where $\chi_{eff,s}$ is the average segmental interaction parameter of the copolymers α and β (χ_{eff}) at the spinodal point and χ_{eff} is defined by

$$\chi_{eff} \equiv \chi_{SI}(f_\alpha - f_\beta)^2 \quad (5)$$

with χ_{SI} being the Flory interaction parameter between the polystyrene and polyisoprene segments. Since $\chi_{eff} \cong \chi_{SI} \times 10^{-4} \cong 10^{-5} \ll \chi_{eff,s} \cong (1/N_\alpha) + (1/N_\beta) \cong 10^{-3}$ for the 50/50 mixtures of $(S\text{-}I)_\alpha/(S\text{-}I)_\beta$, the mixtures cannot undergo the macrophase separation but undergo the microphase separation only. Moreover, since they have $r < 2$, they may not be affected by *the fluctuation-induced segregation effect*[2] and hence by the *macrophase separation induced by microphase separation*, as in the case of the lamellar S-I copolymers with small r. Thus the two S-I copolymers, B1 and B2, are mixed with each other at the molecular level to form a single microdomain morphology.

Figure 7 shows the Bragg spacing of the first-order peaks D (open circles) and the average radius R of the spheres or cylinders (filled circles) determined from the SAXS profiles shown in Figure 5 as a function of weight fraction of the larger block copolymer B2. R was determined with eq 3 for spheres and eq 2 for cylinders. It should be noted that there is a significant change of R with the weight fraction of B2 for both the spheres and the cylinders even if the error bars are taken into account. It is natural that the cylinder radius R increases with the increasing weight fraction of copolymer B2 having the larger molecular weight than B1. However, it is a surprise that and is not well understood at present why the sphere radius R decreases with increasing copolymer B2 weight fraction.

B. Miscible Blends of HK5/BSI9 with $r < r_c$ and with Mismatched Composition ($f_\alpha \cong 1 - f_\beta \cong 0.7$): Microphase Separation Only. The mixtures of HK5/BSI9 have a considerably large mismatch in the compositions f_{PS} ($|f_\alpha - f_\beta| = 0.38$) so that $\chi_{eff} \cong \chi_{SI} \times 0.14$ can be as large as about 1.4×10^{-2}, because $\chi_{SI} \cong 0.1$ at 100 °C in bulk. As the concentration increases during the solvent evaporation process, χ_{eff} increases and approaches the critical value for the microphase separation or the macrophase separation. For such systems as these mixtures, the self-assembled structure is crucially affected by the instability which occurs first, i.e., instability for macrophase separation or for microphase separation. To answer this question, we made the stability analysis as described earlier,[2] the results of which are shown in Figure 8. Here $\chi_{s,macro}$ and $\chi_{s,micro}$ are the χ_{eff} values at which the

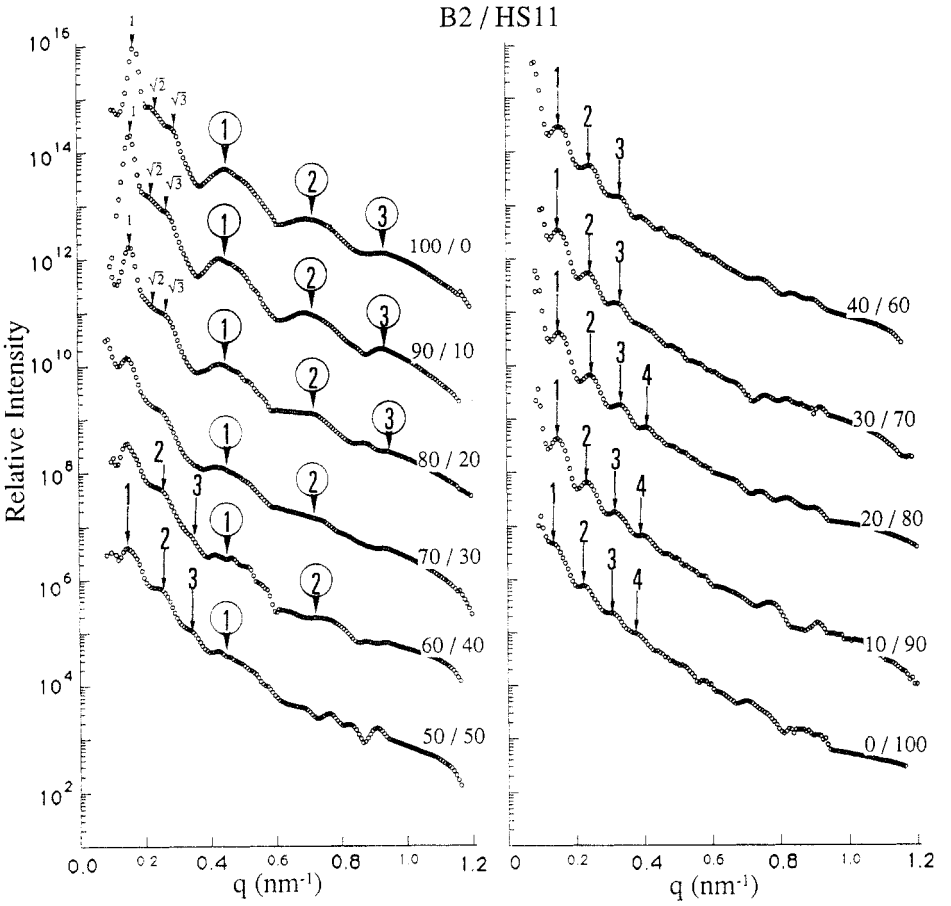

Figure 6. SAXS profiles obtained for the mixtures of B2/HS11 with the compositions 100/0, 90/10, 80/20, 70/30, 60/40, 50/50, 40/60, 30/70, 20/80, 10/90, and 0/100.

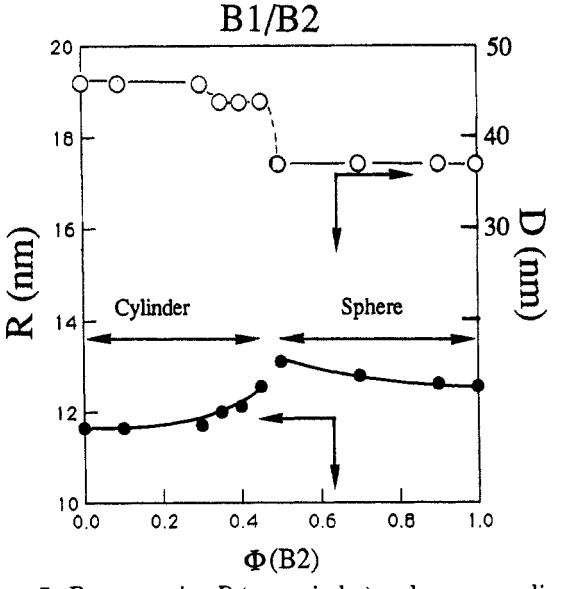

Figure 7. Bragg spacing D (open circles) and average radius of PI spheres or PI cylinders R (filled circles) for the binary mixtures of B1/B2 determined from SAXS measurements as a function of the weight fraction of the larger block copolymer B2.

system becomes unstable for the macrophase and microphase transitions, respectively, i.e.,

$$I^{-1}(q_m) \sim S(q_m)/W(q_m) - 2\chi_{eff,s} = 0 \quad (6)$$

$$\chi_{eff,s} \equiv \chi_{s,macro} \quad \text{in the case when } q_m = 0 \quad (7)$$

$$\chi_{eff,s} \equiv \chi_{s,micro} \quad \text{in the case when } q_m \neq 0 \quad (8)$$

where q_m is the magnitude of the scattering vector at which

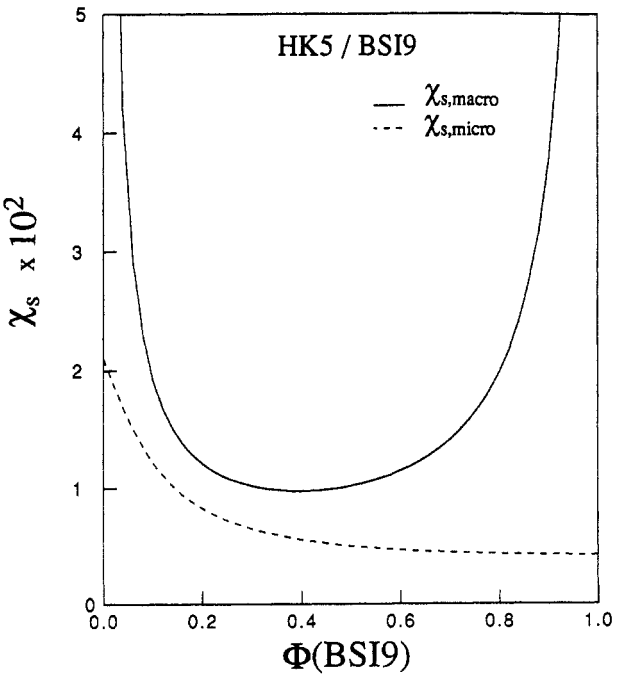

Figure 8. Thermodynamic stability limits calculated for the macrophase (solid curve) and microphase transition (broken curve) for the binary mixtures of HK5/BSI9.

the scattered intensity becomes maximum. $S(q)/W(q)$ is the function defined previously[2] and depends only on the conformation of polymer chains.

The result shown in Figure 8 indicates that $\chi_{s,micro} < \chi_{s,macro}$ for all compositions. As the concentration of the system increases from the disordered state during the solvent evaporation process, χ_{eff} increases from a value smaller than $\chi_{s,micro}$ and eventually reaches $\chi_{s,micro}$. There-

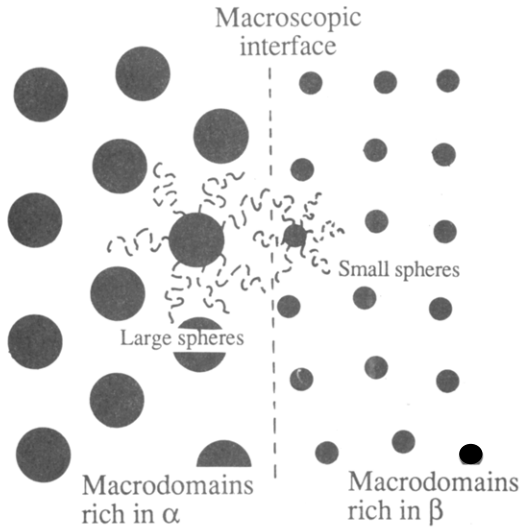

Figure 9. Schematic illustration for the macrophase separation between large and small spherical microdomains.

fore, the microphase separation should always occur prior to the macrophase separation during the solvent evaporation process. Once the microphase separation occurs, the spinodal curve for the macrophase separation loses its physical significance and the microphase separation may control the final morphology observed in the solvent-cast films. Moreover, since the mixture has $r < 3$, the *fluctuation-induced segregation effect* is weak so that the microphase separation is not expected to induce the macrophase separation.

C. Immiscible Blends of B2/HS11 with $r > r_c$ and $f_\alpha \cong f_\beta \cong 0.8$: Macrophase Separation Induced by Microphase Separation. Copolymers HS11 and B2 have nearly matched compositions $|f_\alpha - f_\beta| = 0.05 \ll 1$, as in the case of B1/B2. Therefore, the mixtures of B2/HS11 are not expected to undergo the macrophase separation. Nevertheless, they underwent macrophase separation into the large and small spheres for $0 < \Phi_\alpha < 0.8$, as shown in Figure 3, although this macrophase separation is limited to the *mesoscopic scale*, i.e., on the order of the microdomain size, but never results in formation of the macrodomains of the large spheres and of the small spheres, as schematically shown in Figure 9. This evidence that the macrophase separation of the spherical system extends only to the *local or the mesoscopic scale* but not to the macroscopic scale is in good contrast with the macrophase separation in the lamellar block copolymer systems studied previously.[1,2] Figure 10 shows a typical TEM micrograph of a binary mixture of HY12 (denoted α)/HY8 (denoted β) 50/50 wt %/wt % with $f_\alpha \cong f_\beta \cong 0.5$ and $r \cong 16$.[1] In this micrograph we observe dispersed macrophases of β in the matrix of α. The micrograph clearly shows that the two copolymers underwent the macrophase separation to form macrodomains of the thick lamellae (rich in α) and of the thin lamellae (rich in β). The corresponding macrophase separation in our spherical systems would be the one schematically illustrated in Figure 9 in which there are macrodomains composed of the large spheres in a cubic lattice and of the small spheres also in a cubic lattice. However, this kind of conventional macrophase separation was not observed so far in the real spherical systems (Figure 3). The "*local*" macrophase separation generates more or less a random mixing of the large and small spheres, as schematically shown in Figure 16c later (and as found for $0.5 \leq \Phi_\alpha \leq 0.7$ in Figure 3), or the large spheres dispersed in a cubic lattice of the small spheres, as schematically shown in Figure 17c later (and as found for $\Phi_\alpha = 0.1$ in Figure 3).

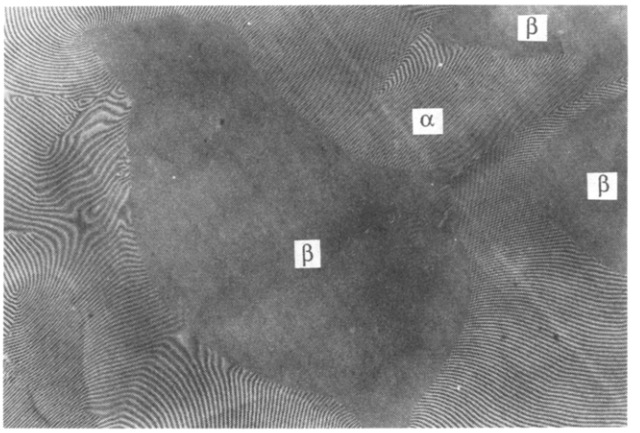

Figure 10. Transmission electron micrograph of the ultrathin section of the binary mixture of $(S\text{-}I)_\alpha/(S\text{-}I)_\beta$ (HY8/HY12) 50/50 wt %/wt % with $f_\alpha \cong f_\beta \cong 0.5$ and $r \cong 16$. This mixture shows the macrophase separation of β-rich macrodomains dispersed in the α-rich matrix. The α and β macrodomains are composed of alternating lamellar microdomains with large and small spacings, respectively.

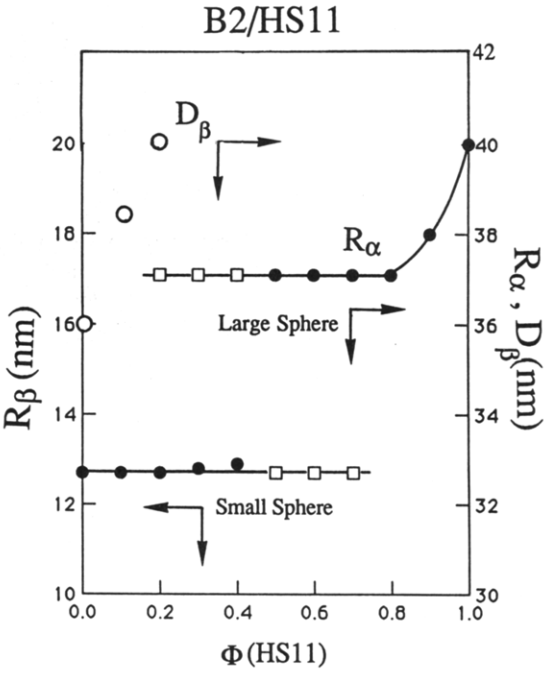

Figure 11. Average radii of PI spheres R_α and R_β (filled circles) for the binary mixtures of B2/HS11 determined from SAXS measurements as a function of the weight fraction of the larger block copolymer $(S\text{-}I)_\alpha$ (HS11).

Figure 11 shows the average radius of the spheres R as determined with eq 3 and the Bragg spacing D_β of the spheres as determined from the first-order peak position $q_{m1,\beta}$,

$$D_\beta = 2\pi/q_{m1,\beta} \tag{9}$$

Concerning the average radii of the spheres R_α and R_β, the data points marked by filled circles were directly determined from the peak positions shown in Figure 6 and the data points marked by open squares were estimated by the curve-fitting with eq 13 as will be discussed later.

As in the case of the binary mixtures of the lamella-forming copolymers, the large copolymer α can solubilize the small copolymer β up to the critical amount $\Phi_{\beta,C} \equiv 1 - \Phi_{\alpha,CL}$ so that the two copolymers are mixed at the molecular level, forming a single spherical microdomain structure in the composition range satisfying

$$\Phi_\alpha > \Phi_{\alpha,CL} \quad \text{or} \quad \Phi_\alpha < \Phi_{\alpha,CS} \tag{10}$$

where the critical concentrations for the spherical systems are

$$\Phi_{\beta,C} = 1 - \Phi_{\alpha,CL} \cong 0.2 \tag{11}$$

as shown in Figure 11, and $\Phi_{\alpha,CS} \cong 0$; i.e., the small spheres composed of the small copolymers β hardly solubilize the large copolymers α. Note that the critical concentration $\Phi_{\beta,C}$ is smaller than that for the lamellae, which was about 0.3.[1] As in the binary mixtures of the lamella-forming copolymers,[1] the large and small spheres coexist at

$$\Phi_{\alpha,CS} \leq \Phi_\alpha \leq \Phi_{\alpha,CL} \tag{12}$$

and their average radii, denoted R_α and R_β, are independent of Φ_α. A possible interpretation of eq 12 will be given on the basis of the macrophase separation induced by the microphase separation in section V.

Although the coexistence of the two different sizes of the spheres, R_α and R_β, is not explicitly clear from Figure 6, it can be proven so from the following analysis on the scattering form factors from the spheres for the mixtures (see Figure 12). In this analysis we assume that the sphere form factor per unit volume of the mixture having the composition Φ_α, $I(\Phi_\alpha)$, is given by a sum of that for the large spheres and that for the small spheres,

$$I(\Phi_\alpha) = N_{S\alpha}(\Phi_\alpha)I_\alpha + N_{S\beta}(\Phi_\alpha)I_\beta \tag{13}$$

where N_{SK} is the number of the Kth sphere per unit volume and I_K is the form factor for the Kth isolated sphere (K = α or β). Note that N_{SK} is a function of Φ_K and that experimental evidence given by Figure 3 leads to

$$I(\Phi_\alpha{=}0.8) = N_{S\alpha}(\Phi_\alpha{=}0.8)I_\alpha + N_{S\beta}(\Phi_\alpha{=}0.8)I_\beta = N_{S\alpha}(\Phi_\alpha{=}0.8)I_\alpha \equiv I_{20/80} \tag{14}$$

$$I(\Phi_\alpha{=}0) = N_{S\alpha}(\Phi_\alpha{=}0)I_\alpha + N_{S\beta}(\Phi_\alpha{=}0)I_\beta = N_{S\beta}(\Phi_\alpha{=}0)I_\beta \equiv I_{100/0} \tag{15}$$

where $I_{20/80}$ and $I_{100/0}$ are the form factors for the 20/80 and 100/0 mixtures of B2/HS11 which can be experimentally obtained (Figure 6). The intensity $I_{100/0}$ at small q ($q \leq 0.3\,nm^{-1}$) is clearly affected by intersphere interference and should be affected by the spatial arrangement of the small spheres. This fact should not be overlooked in the following analysis. Here we assume the following: (i) the 20/80 mixtures form the large spheres of radius R_α, (ii) the small spheres of radius R_β do not contain at all the large copolymers α, and (iii) the sizes R_α and R_β are independent of Φ_α for the mixtures undergoing the phase separation (see Figure 11). From eqs 14 and 15 and after some manipulations we obtain

$$I(\Phi_\alpha) = 1.25\Phi_\alpha I_{20/80} + (1 - 1.25\Phi_\alpha)I_{100/0} \tag{16}$$

Figure 12 shows a result of this analysis where the solid lines are the sphere form factor $I(\Phi_\alpha)$ of the mixtures having the composition Φ_α estimated from eq 16. The calculated form factor represents very well the experimental scattering profiles shown by the data points, except for the profiles at small q where the intersphere interference becomes important, and hence the deviations from the sphere form factor are quite naturally expected.

D. Immiscible Blends with Mismatched Compositions ($f_\alpha \cong 1 - f_\beta \cong 0.8$): Superlattice Formation and Macrophase Separation Followed by Microphase Separation. For the 30/70 mixture of TOKI4/B2, the

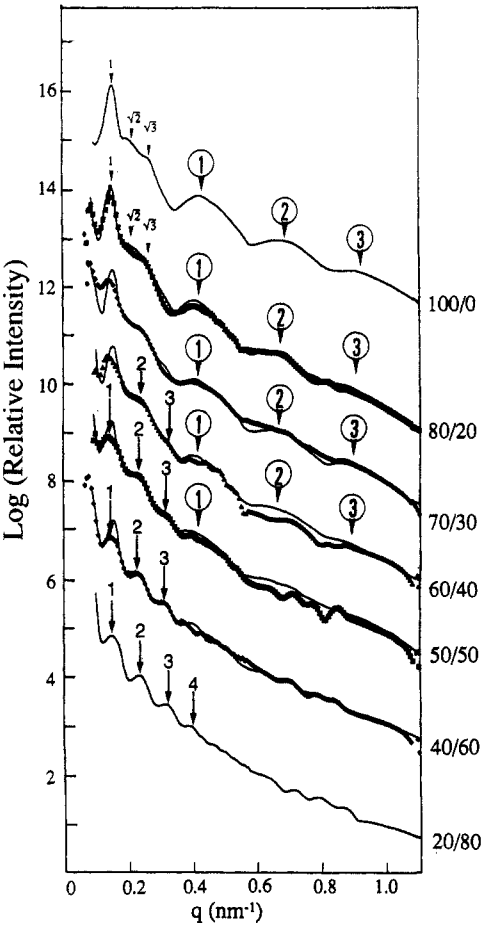

Figure 12. Comparison between the measured SAXS profiles (data points) and the fitted profiles (solid curves) calculated with eq 16.

mismatch of f_{ps} is considerably large $(f_\alpha - f_\beta)^2 = 0.65^2 \cong 4 \times 10^{-1}$ so that $\chi_{eff} \cong 0.4\chi_{SI} \cong 4 \times 10^{-2} > \chi_{eff,s} \cong 1.0 \times 10^{-2}$. Thus the system can be unstable for the macrophase transitions as well as for the microphase transition. The results of the stability analysis show that $\chi_{s,macro} < \chi_{s,micro}$ for this mixture, as shown in Figure 13a. Hence the mixture first undergoes spinodal decomposition (SD), generating the domains rich in α (B2) and rich in β (TOKI4) as shown in Figure 13b. As this macrophase separation progresses and the amplitude of the concentration fluctuation $\Delta\Phi_\alpha$ increases, the domains rich in α will have the local composition Φ_α greater than $\Phi^L{}_{\alpha m}$ and the domains rich in β will have the local composition Φ_α smaller than $\Phi^S{}_{\alpha m}$. The microphase separation starts to occur locally in those domains satisfying $\Phi_\alpha > \Phi^L{}_{\alpha m}$ and $\Phi_\alpha < \Phi^S{}_{\alpha m}$, generating the microdomains similar to the neat α and those similar to the neat β. The microdomain structures thus formed will affect further ordering processes of the systems.

V. Model for Immiscible Blends with $f_\alpha \cong f_\beta$ but $r > r_c$: Macrophase Separation Induced by Microphase Separation

We now discuss a possible qualitative model which may account for the experimental observation on B2/HS11 described in section IV.C, i.e., macrophase separation induced by the microphase separation. The stability analysis based upon RPA indicates that the mixtures become unstable at a particular mode with the wavenumber $q_m \neq 0$ (as shown in Figure 14a). The composition dependence of q_m indicates that this wavenumber is controlled by the large copolymer α (HS11) for $0.3 < \Phi_\alpha < 1$ (the solid line in Figure 14b). This figure includes also the wavenumber q_m for B1/B2, for which q_m gradually decreases with Φ_α (the broken line in Figure 14b).

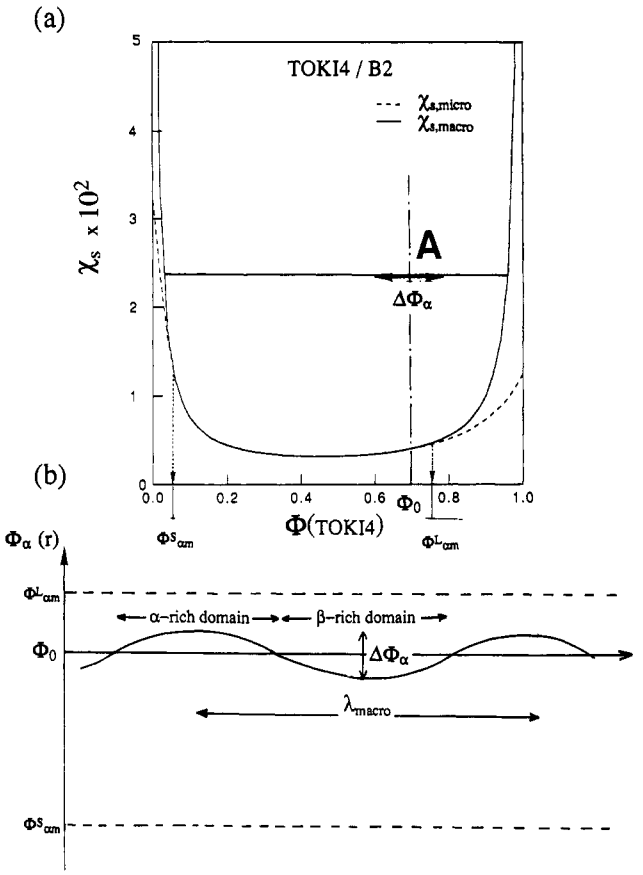

Figure 13. (a) Calculated thermodynamic stability limit for the macrophase (solid curve) and microphase transition (broken curve) for the binary mixtures of TOKI4/B2. Φ^S_{am} and Φ^L_{am} are critical compositions (Lifshitz points) below and above which the microphase transition can occur first, respectively, upon raising the segregation power χ. (b) Schematic illustration of the spatial concentration fluctuation $\Phi_\alpha(r)$ at a given time during the spinodal decomposition at point A in part (a).

Figure 15 schematically illustrates a spatial configuration of copolymers α and β (part a) and spatial concentration fluctuations of polymer segment B (part b) at a particular time in the single-phase mixture. The wavelength of the dominant mode of the fluctuation $2\pi/q_m$ is close to that for neat large copolymer α, as schematically shown in Figure 15b for a mixture with the composition Φ_α of our interest. As the mixture approaches the spinodal point, the amplitude of the fluctuations $\Delta\Phi$ increases. Under this situation the chains of copolymer β labeled $\beta 1$ ($\beta 3$) in Figure 15a are put, respectively, in the situation as if they were put in the fields of homopolymer A_α (B_α). Here A_α and B_α are the block chains A and B of large copolymer α, respectively. Thus they may be subjected to the segregation effect relevant to the mixture $(A\text{-}B)_\beta/A_\alpha$ or $(A\text{-}B)_\beta/B_\alpha$. They may be segregated either out of the field of $(A\text{-}B)_\alpha$ or to the interfacial region between A_α-rich and B_α-rich domains with their A_β and B_β chains oriented toward the respective domains of α, as schematically shown for the chain of copolymer β labeled $\beta 2$ in Figure 15a. This is the *fluctuation-induced segregation effect* which may give the basis for the interpretation of the macrophase separation induced by the microphase separation, i.e., the same effect as introduced previously to explain the macrophase separation of the lamella-forming copolymers.[2] As in the case of the lamella-forming copolymer mixtures, only a limiting amount of copolymer β can be solubilized in the domains of copolymer α in such a configuration as shown for the copolymer chain labeled $\beta 2$, in the segregation limit. This limiting amount may be equal to $\Phi_{\beta,C} \equiv 1 - \Phi_{\alpha,CL} \cong 0.2$ for the sphere-forming copolymer mixtures

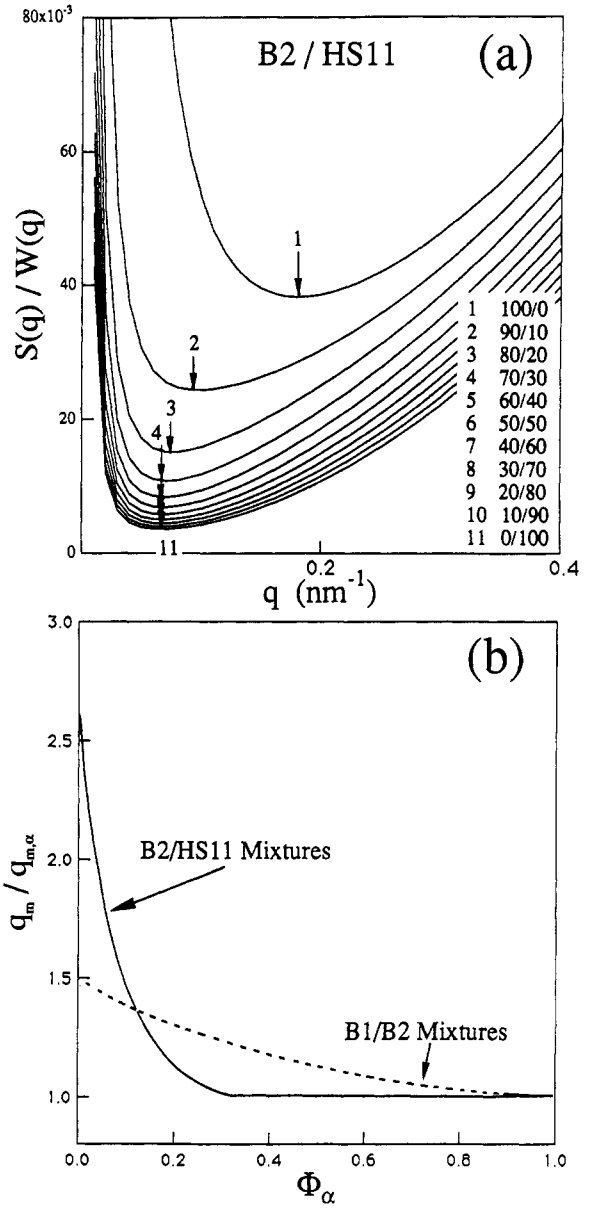

Figure 14. (a) RPA prediction of the thermodynamic force $S(q)/W(q)$ required to generate the q-Fourier mode of the concentration fluctuations when $\chi = 0$ for the binary mixtures of B2/HS11. The composition Φ_α of the large molecular weight copolymer α is changed from 0 to 1. (b) Predicted composition dependence of the wavenumber q_m which becomes unstable for the binary mixtures of B2/HS11 (the solid curve) and B1/B2 (the broken curve). The value q_m for the B2/HS11 mixtures is controlled by the large copolymer α (HS11) for $0.3 < \Phi_\alpha$, while that for the B1/B2 mixture gradually decreases with Φ_α. $q_{m,\alpha}$ is the wavenumber for neat copolymers α.

and may be controlled by the cost of the stretching free energy of copolymers α and β on packing their A and B block chains in the respective domains with their chemical junctions at the interfaces.

Small copolymer β to the amount of $(\Phi_\beta - \Phi_{\beta C})$, which is segregated out from the field of the large copolymer α due to the fluctuation-induced segregation effect, should have such a spatial distribution as schematically illustrated in Figure 16 or 17, depending upon the composition of the α/β mixtures. Figure 16 shows a mixture rich in large copolymer α, and hence the corona block chains A_α are overlapping each other in a segregation situation where α forms the microdomains but the segregated-out small copolymer β is still in the disordered state (part a). On the other hand, Figure 17 shows a mixture rich in small copolymer β, and hence the corona chains A_α are not overlapping one another (part a).

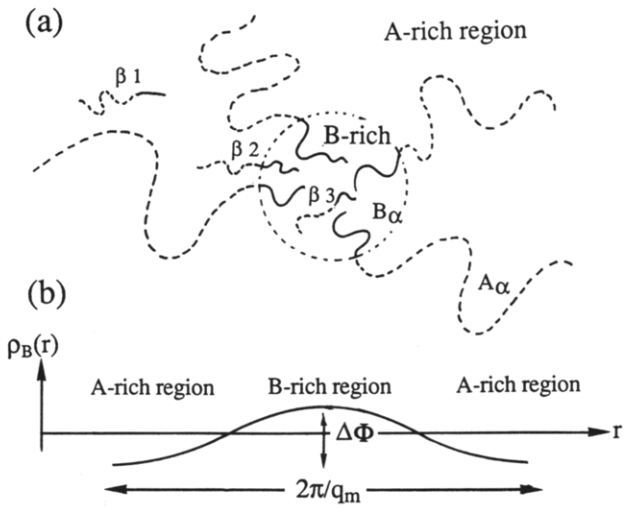

Figure 15. (a) Schematic illustration of the spatial distribution of the large and small copolymers α and β in the single phase mixture near the spinodal point and (b) spatial variation in the concentration of segments B, $\rho_B(r)$, of A–B diblock copolymers. According to RPA prediction, the wavelength of the dominant mode of the fluctuations, $2\pi/q_m$, is close to that for the neat large block copolymer α.

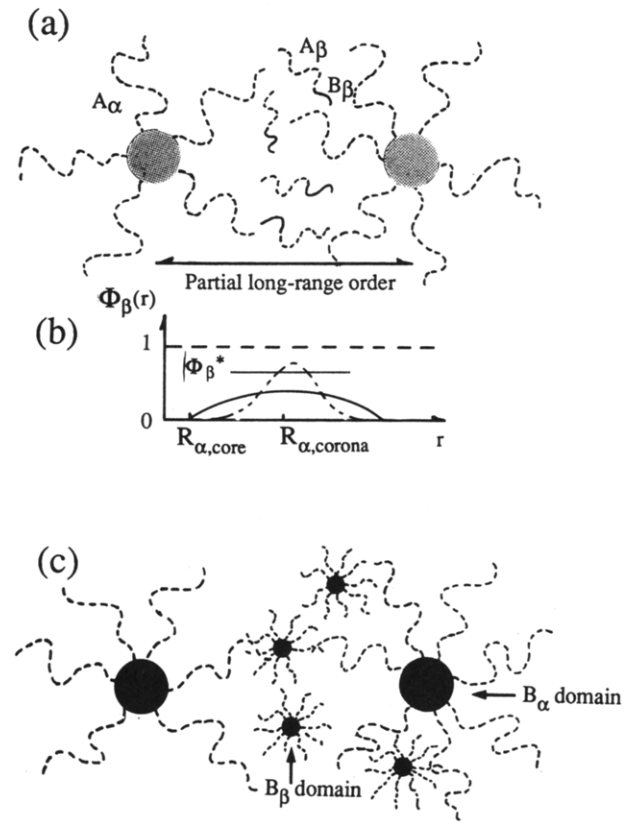

Figure 16. (a) Schematic illustration of the spatial distribution of the large and small block copolymers, α and β, after the fluctuation-induced segregation for the mixtures rich in the large copolymers α. (b) Spatial distribution of the small block copolymers β between two large spherical micelles corresponding to part (a). (c) Schematic illustration of the coexistence of large and small spherical micelles. There is a partial, long-range order for the large micelles.

In the overlapping situation, Figure 16b schematically shows a spatial concentration variation of copolymer β, $\Phi_\beta(r)$. $\Phi_\beta(r)$ increases from nearly 0 at $r = R_{\alpha,\text{core}}$, the core radius of α-rich domains, to a maximum at $r = R_{\alpha,\text{corona}}$, the radius of the corona of α-rich domains, but the maximum value is smaller than unity as schematically shown by the solid line in (b). As the segregation power between A and B increases, $\Phi_\beta(r)$ biases more toward the

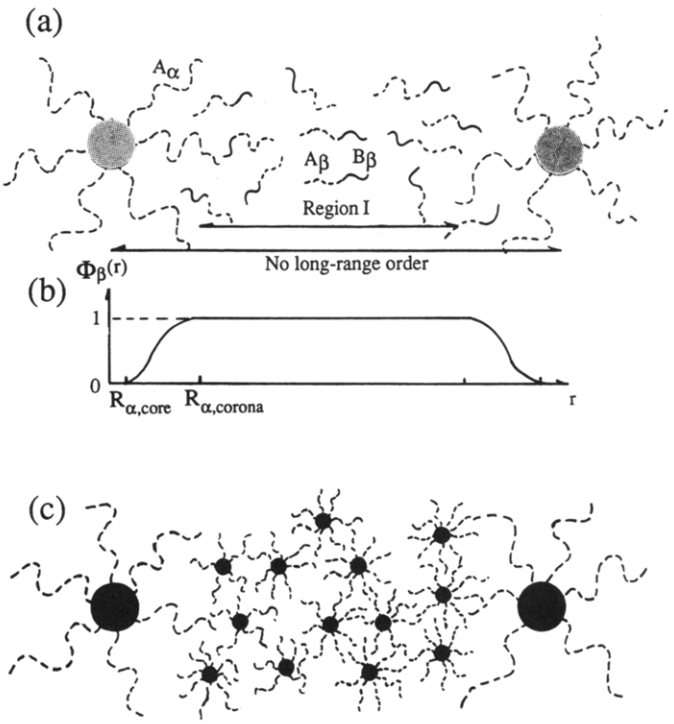

Figure 17. (a) Schematic illustration of the spatial distribution of the large and small block copolymers, α and β, after the fluctuation-induced segregation for the mixtures rich in the small copolymers β. (B) Spatial distribution of the small block copolymers β between two large spherical micelles corresponding to (a). (c) Schematic illustration of the coexistence of large and small spherical micelles. There is no long-range order for the large micelles.

center between the two B-rich spheres, as drawn by the broken line, and $(A\text{-}B)_\beta$ starts to undergo the microphase separation in the region where $\Phi_\beta(r)$ becomes greater than the critical concentration Φ_β^*. As the segregation power further increases, $\Phi_\beta(r)$ should have a sharper spatial distribution centered at $r = R_{\alpha,\text{corona}}$ and Φ_β^* decreases, so that the microphase separation of $(A\text{-}B)_\beta$ further progresses toward the inner side of the corona, i.e., from $r \cong R_{\alpha,\text{corona}}$ to $r = R_{\alpha,\text{core}}$, resulting in the microdomain formation of copolymer β, as schematically shown in part c of Figure 16.

The other possibility is that copolymer β is completely segregated out from the domains of copolymer α to result first in the macrophase separation between the ordered cubic lattice rich in α and the disordered phase of β and then in the microphase separation of the β phase into the cubic lattice to end up with the structure schematically shown in Figure 9. Which becomes the final structure, the one schematically shown in Figure 16c or the one in Figure 9, depends on the segregation power between $(A\text{-}B)_\beta$ and A_α and on the competition of the two rates, i.e., the rate of translational diffusion of copolymer β and the rate of microphase separation of β under a given solvent evaporation condition.

In the nonoverlapping situation, the spatial concentration variation of small copolymer β before its microphase separation may be represented schematically by parts a and b in Figure 17. As the segregation power between A and B chains increases, microphase separation of β starts to occur from the **interstitial** region between the peripheries of the neighboring A_α corona, i.e., region I in Figure 17a. Upon a further increase in the segregation power, the microphase separation front moves toward the inside of the corona, resulting in the microdomain structure shown in Figure 17c. Again one can think of the possibility of forming the macrophase-separated structure illustrated in Figure 9, the realization of which again depends on the

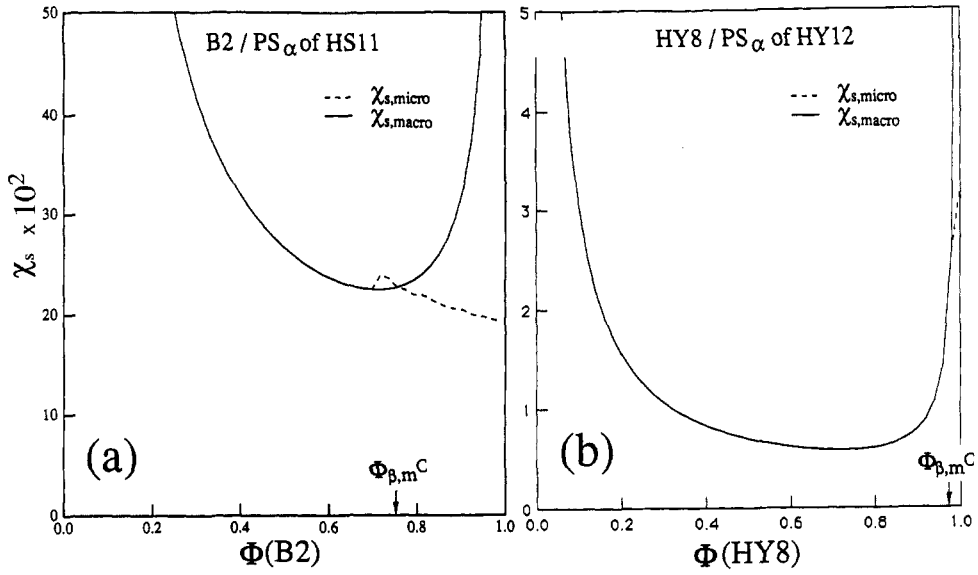

Figure 18. Predicted thermodynamic stability limits for the macrophase (solid curves) and microphase transition (broken curves) for the binary mixtures of (a) B2/(PS_α of HS11) and (b) HY8/(PS_α of HY12).

segregation power and the competition of the two rates: one is the translational diffusion rate of the large spheres to form their macrodomains in a cubic lattice and the other is the rate of the microphase separation of small copolymer β.

How can we explain the difference between the morphologies of the lamella-forming and sphere-forming copolymer mixtures, i.e., the "locally" macrophase-separated structure as shown in Figures 16c and 17c vs the "macroscopically" macrophase-separated structure as shown in Figure 10? A possible interpretation may be done on the basis of a difference in the fluctuation-induced segregation effect. The most important part of this argument may be exaggerated by considering the difference between the segregation behaviors of $(S\text{-}I)_\beta/PS_\alpha$ mixtures relevant to the two mixtures, B2/HS11 and HY8/HY12, where PS_α denotes a PS homopolymer having the same molecular weight as the PS block chains in large copolymer $(S\text{-}I)_\alpha$ (see the situations shown in Figure 15 of this paper and in Figure 12 of ref 2). Figure 18 shows the RPA analysis of $(S\text{-}I)_\beta/PS_\alpha$ relevant to B-2/HS-11 (i.e., a binary mixture of B-2 and PS_α for HS11, part a) and that relevant to HY8/HY12 (i.e., a binary mixture of HY8 and PS_α for HY12, part b). The two systems are clearly different in the following points: (i) the critical concentration $\Phi_{\beta,m}{}^C$ above which microphase separation occurs is much lower in the sphere-forming mixture (part a) than in the lamella-forming mixture (part b), and (ii) microphase separation occurs prior to the macrophase separation with increasing segregation power in the former system, while the situation is reversed in the latter system. These differences may explain the difference in the final structures of the two systems.

VI. Conclusion

The structure self-assembly in binary mixtures of SI diblock copolymers which form spherical or cylindrical microdomains was studied. In the case when the two copolymers have matched compositions, $f_\alpha \cong f_\beta \cong 0.2$, the following two cases are found: (i) two copolymers are mixed at the molecular level for all compositions to form a single domain morphology (either spheres or cylinders) if $r \equiv N_\alpha/N_\beta \leq 2$ (see section IV.A) and (ii) if $r \geq 7$, they are partially miscible; they are miscible at biased compositions $\Phi_\alpha \geq \Phi_{\alpha,CL}$ or $\Phi_\alpha \leq \Phi_{\alpha,CS}$ with $\Phi_{\alpha,CL} \cong 0.8$ and $\Phi_{\alpha,CS} \cong 0$ (i.e., large copolymer α can solubilize small copolymer β up to about 20% in its domains, but the small copolymer can hardly solubilize the large copolymer), or they undergo the phase separation into α-rich spheres and spheres composed of almost pure β at $\Phi_{\alpha,CS} < \Phi_\alpha < \Phi_{\alpha,CL}$ (section IV.C). In the latter case, the α-rich spheres are more or less randomly mixed with the β spheres packed in a distorted lattice at $0.5 \leq \Phi_\alpha \leq 0.8$ or with the β spheres packed in the cubic lattice at $0 < \Phi_\alpha < 0.5$. In both cases the macrophase separation in the sphere-forming copolymer mixtures did not result in the macrodomains of the α spheres and β spheres as schematically shown in Figure 9, but resulted in the rather locally macrophase-separated structure as shown in Figure 3 or schematically shown in Figures 16c and 17c. This macrophase separation is proposed to be induced by the microphase separation: the macrophase separation may be triggered by the fluctuation-induced segregation effect (Figure 15) when the segregation power between the PS and PI chains becomes greater than that corresponding to the spinodal point (section V).

In the case when the two copolymers have such mismatched compositions as $f_\alpha \cong 1 - f_\beta \cong 0.3$ or $f_\alpha \cong 1 - f_\beta \cong 0.2$, their mixture shows either a uniform mixing at a molecular level forming a single microdomain morphology with long-range order (Figure 2) or a *modulated* or *superlattice* structure with dual morphological entities with different characteristic length scales (Figure 4): (i) the macrodomains rich in α and those rich in β have a micron length scale and (ii) the microdomains corresponding to the α and β copolymers have a nanometer length scale. The superlattice structure is proposed to be formed by the macrophase separation followed by the microphase separation (section IV.D).

Acknowledgment. The authors are grateful to Prof. Fumihiko Tanaka for his useful discussions. This work was supported in part by a Grant-in-Aid for Scientific Research (05650673) from the Ministry of Education, Science, and Culture, Japan.

References and Notes

(1) Hashimoto, T.; Yamasaki, K.; Koizumi, S.; Hasegawa, H. *Macromolecules* **1993**, *26*, 2895 and references cited therein.

(2) Hashimoto, T.; Yamasaki, K.; Koizumi, S.; Hasegawa, H. *Macromolcules* **1994**, *27*, 1562 and references cited therein.